Physicochem. Probl. Miner. Process., 55(1), 2019, 196-207

http://www.journalssystem.com/ppmp

Physicochemical Problems of Mineral Processing

ISSN 1643-1049

Received March 5, 2018; reviewed; accepted April 24, 2018

Removal of quinoline using various particle sizes anthracite: adsorption kinetics and adsorption isotherms

Hongxiang Xu, Xianfeng Sun*, Yuexian Yu, Guowei Liu, Liqiang Ma, Gen Huang

School of Chemical Engineering and Technology, China University of Mining & Technology (Beijing), Beijing 100083, China

Corresponding author: sunxianfeng1025@outlook.com (X.F. Sun)

Abstract: This work provided an adsorption method of the removal of quinoline by using anthracite of various particle sizes. The characteristics of the adsorbents were analyzed by Camsizer XT for particle size analysis, FT-IR for functional groups, X-ray diffusion for mineralogical composition, Brunauer-Emmett-Teller for specific surface area and Barrett-Joyner-Halenda for pore size distribution. The average particle size of AC1-AC4 were 0.0342 mm, 0.1015 mm, 0.2103 mm and 0.3815 mm, respectively. The specific surface of the AC1-AC4 were 3.5 $m^2 \cdot g^{-1}$, 1.5 $m^2 \cdot g^{-1}$, 0.7 $m^2 \cdot g^{-1}$ and 0.1 $m^2 \cdot g^{-1}$ respectively. The adsorption capacity present a linear increase with the specific surface area increasing. To reveal the process of the adsorption, the adsorption kinetics and isotherms were performed. The kinetics data were analyzed by pseudo-first-order, pseudo-second-order and intra-particle diffusion equation using linearized correlation coefficient. Pseudo-second-order was found to best represent the kinetics data, which indicated that the adsorption of quinoline onto anthracite belongs to chemisorption. The equilibrium isotherms data were analyzed by Langmuir model and Freundlich model, the results indicated that the Freundlich model fit well for all the adsorption processes, which showed that the adsorption of quinoline onto anthracite belongs to endothermic reaction.

Keywords: adsorption isotherm, anthracite, particle size, quinoline adsorption kinetics

1. Introduction

There is a little of quinoline in wastewater, but it is far more than the integrated wastewater discharge standard, especially in coking wastewater. Quinoline and its derivatives are mutagenic, carcinogenic and toxic, so they have the potential to heavily pollute soil and water (Sutton et al. 1996). Thus, it is essential to removal such organic contaminants from wastewater. Biological treatment of wastewater is used to reduce the environmental impact of discharge. However, previous studies have demonstrated that the method is not able to meet the standard for discharge of water (Burmistrz et al. 2014). And the discharge water after biological treatment still contains the residual amount of oxygen-consuming substances (Magnus et al. 2000).

Adsorption is a widely used method for treating wastewater. Activated carbon is the most widely and effectively used absorbent (Zhu 2001), with a porous structure provides a large surface area and a good capacity for adsorbing organic molecules by a variety of physicochemical mechanisms and forces. Some studies indicated that activated carbon achieves great effect on adsorbing dye, lignin, phenol, quinoline, pyridine, indole and other organic pollutants (Andersson et al. 2011b, Başar 2006, Carvajal-Bernal et al. 2015, Fletcher et al. 2007). However, the usage of activated carbon is limited by its high cost and difficult regeneration (Aksu and Yener 2001, Badmus and Audu 2009).

Coal, as a natural polyporous materials possessing a relative large surface area, stepped into researcher's sight. Xia et al. (2000) found that sulfonated lignite had great capacity to adsorb heavy metal ion in wastewater. Cai et al. studied that coking coal adsorbed main organic pollutants from coking wastewater and the results indicated that the removal efficiency was high (Cai and Tang 2012, Cai et al.

DOI: 10.5277/ppmp18121

2010). The investigation from Fang et al. showed that coal adsorbs organic pollutants preferentially (Fang et al. 2010). The weathered coal had great adsorption capacity in a wide range of pH and the removal efficiency of copper was 60~70% (Yi 2012). Because of the hydrogen-boning, the capacity of lignite to adsorb phenol was much larger than that generally observed with activated carbons when normalized for the surface areas (Polat et al. 2006).

There are several advantages of coal as adsorbent to treat cooking wastewater. The coal is easily available, abundant and cheap. The value of coal will not reduce after adsorbing organic pollutants. The coking plant is usually built together with coal preparation plant, which can save transportation costs.

The aim of this work is to investigate the characteristics of adsorbing quinoline on anthracite with various particle sizes and provide the basis for coal as adsorbent. The adsorbents were characterized by Camsizer XT particle size analysis, Brunauer–Emmett–Teller surface area analysis, Barrett-Joyner-Halenda pore size distribution, Fourier-transform infrared spectroscopy and X-ray diffraction. The adsorption behavior was investigated by adsorption kinetics and adsorption equilibrium. The results of this research are expected to provide a more detailed adsorption process of various particle anthracite.

2. Materials and methods

2.1. Materials

The anthracite used in this study was obtained from a coal preparation plant in Xuzhou, Jiangsu province, China. The coal samples belong to concentration of gravity separation with a particle size less than 50 mm, and then they were crushed and grinded to below 0.5 mm by jaw crush and ball mill, respectively. Finally, the grinded samples were screened using a mechanical sieve shaker with 0.25 mm, 0.125 mm, 0.074 mm pore size, respectively. All samples were dried in an oven at 105℃ to a constant weight.

2.2. Samples characterization

Particle size of the four samples were measured by Camsizer XT (Germany). About 1.0 g dry coal were put on the feeding cell to analyse the particle size.

Infrared spectra of all adsorbents were recorded between 4000 and 400cm^{-1} in a VERTEX70V FTIR (Germany) instrument. Pellets were prepared by compressing mixtures of 0.5% finely ground anthracite with KBr.

X-ray diffraction of the anthracite samples were conducted between 3 and 70 deg by X-ray diffraction (XRD, Rigaku D/max 2500 V, Target = Cu, Step width = 0.02, operating at an acceleration voltage of 40 kV.).

The specific surface area properties of the coals were determined by measuring the adsorption of nitrogen at 77 K on a BELSORP-minill BET (Japan). The samples were dried for 24 h at 350℃ in nitrogen gas prior to analyse. The specific surface area was calculated using the Brunauer-Emmett-Teller model(Kaya et al. 2013b), and the pore size distribution was conducted by Barrett-Joyner-Halenda model(Barrett et al. 1951).

2.3. Bath adsorption tests

Batch experiments were performed to study the effects of initial adsorbate concentration, the adsorption time and experiment temperature on adsorption process. For each experiment run, aqueous solution of quinoline was prepared by dissolving the analytical reagent in deionized water. The 50 cm^3 quinoline solution and 2.0000 g anthracite were taken into 100 cm^3 stoppered conical flask. This mixture was mounted on a temperature-controlled shaking water bath at a constant speed of 120 rpm. All samples were filtered to remove the adsorbents with 0.045μm pore size. The filtrate concentration was determined by UV adsorption and calculated using the formula:

$$q_t = \frac{C_0 - C_t}{m} \tag{1}$$

where q_t (mg·g^{-1}) is the quinoline removed at time t by a unit mass of adsorbent, C_0 (mg·dm^{-3}) is the initial quinoline concentration, C_t (mg·dm^{-3}) is quinoline concentration at time t, and m (g·dm^{-3}) is the amount of adsorbent added.

To observe the effect of the adsorption time on anthracite removing quinoline and to collect kinetics data, parallel experiments were performed in various time from 10 minutes to 180 minutes. The concentration of initial quinoline was 50 mg·dm^{-3}.

To observe the effect of the adsorbate concentration on anthracite removing quinoline and to collect equilibrium isotherm data, parallel experiments were performed in water bath at 25℃ and 50℃, respectively. The concentrations of initial quinoline were 10, 20, 30, 40, 50 mg·dm^{-3}.

To reduce the interference of leachate from coal, the blank experiences should be performed, in which distill water replace quinoline solution. Other processes were same and the filtrate was reference solution.

Using UV/VIS spectrophotometer (Mei Puda 3500 made in China), a calibration curve between UV-absorbance and the standard quinoline concentrations was made at 278 nm (which is the primary absorption peak position for quinoline). The concentration of quinoline was determined by comparing the absorbance values of different coal samples with the standard calibration curve.

2.4. Kinetics analysis

In order to investigate the adsorption process of quinoline on anthracite, three kinetic models were employed to fit the data obtained.

2.4.1. Pseudo-first-order model

The pseudo-first-order model indicates that the adsorption process is controlled by internal mass transfer. Gerente et al.(Gerente et al. 2007a) stated that this model was generally restricted to only the initial 20~40% of the adsorption needed further modifications for longer sorption times and higher fraction surface coverage. The pseudo-fist-order equation model can be represented in the following form(Badmus and Audu 2009):

$$\frac{dq_t}{dt} = \mathrm{K_1}(\mathrm{q_e} - q_t) \tag{2}$$

where q_t is the amount of adsorbate adsorbed at time t (mg·g^{-1}), $\mathrm{q_e}$ the adsorption capacity at equilibrium (mg·g^{-1}), $\mathrm{K_1}$ the pseudo-fist-order rate constant (min^{-1}) and t is the constant time (min). The integration of Eqn. (2) with the initial condition, q_t =0 at t =0 leads to (Gerente et al. 2007b):

$$\log(\mathrm{q_e} - q_t) = \log\mathrm{q_e} - \frac{\mathrm{K_1}}{2.303}t \tag{3}$$

The values of adsorption rate constant ($\mathrm{K_1}$) for quinoline were determined from the plot of log ($\mathrm{q_e}$—q_t) versus t.

2.4.2. Pseudo-second-order model

According to Ho and McKay(Ho and Mckay 1999), chemisorption is involved in the rate-limited step in sorption systems following the pseudo-second-order model. The pseudo-second-order is given as(Badmus and Audu 2009):

$$\frac{dq_t}{dt} = \mathrm{K_2}(\mathrm{q_e} - q_t)^2 \tag{4}$$

where $\mathrm{K_2}$ is the pseudo-second-order rate constant (g·mg^{-1}·min^{-1}). Integrating Eq. (4) and noting that q_t =0 at t =0, the following equation is obtained:

$$\frac{t}{q_t} = \frac{1}{\mathrm{K_2 q_e}^2} + \frac{1}{\mathrm{q_e}}t \tag{5}$$

The initial sorption rate h (mg·g^{-1}·min^{-1}), at $t \to 0$ is defined as:

$$\mathrm{h} = \mathrm{K_2 q_e}^2 \tag{6}$$

2.4.3. Intra-particle diffusion study

The intra-particle diffusion equation can verify presence or absence of intra-particle diffusion and determine whether intra-particle diffusion is the rate-limiting step for adsorption (Mohan and Karthikeyan 1997, Srivastava et al. 2005). The Intra-particle diffusion model is given as (Badmus and

Audu 2009):

$$q_t = \mathrm{K}_3 t^{0.5} + \mathrm{I} \tag{7}$$

where K_3 is the intra-particle diffusion rate constant (mg·g^{-1}·min$^{-0.5}$) and I is the intercept (mg·g^{-1}). According to Eq. (7), a plot of q_t versus $t^{0.5}$ should be a straight line with a slope K_3 and intercept I when adsorption mechanism follows the intra-particle diffusion process.

2.5. Adsorption equilibrium study

To optimize the design of an adsorption system for the adsorption of adsorbates, it is important to establish the most appropriate correlation for the equilibrium curves. Various isotherm equations have been used to describe the equilibrium characteristics of adsorption.

2.5.1. Langmuir isotherm

The Langmuir theory the basic assumption is that the sorption takes place at specific homogeneous sites within the adsorbent(Ho et al. 2002). The Langmuir model is given below:

$$q_e = \frac{\mathrm{K_L q_m} C_e}{1+\mathrm{K_L} C_e} \text{ or } \frac{C_e}{q_e} = \frac{C_e}{\mathrm{q_m}} + \frac{1}{\mathrm{K_L q_m}} \tag{8}$$

where K_L the Langmuir adsorption constant (dm^3·mg^{-1}) relates to the energy of adsorption and q_m signifies adsorption capacity (mg·g^{-1}).

2.5.2. Freundlich isotherm

The Freundlich isotherm is derived by assuming a heterogeneous surface with a non-uniform distribution of heat of adsorption over the surface (Chatzopoulos et al. 1993). The Freundlich model is given below:

$$q_e = K_F {C_e}^{1/n} \text{ or } \log q_e = \log K_F + \frac{1}{n}\log C_e \tag{9}$$

where K_F is the Freundlich constant (dm^3·mg^{-1}), $1/n$ the heterogeneity factor.

3. Results and discussion

3.1. Characterization of adsorbents

The particle size of AC1-AC4 were showed in the Fig. 1. Regarding AC1, the particle size is less than 0.090 mm and distributing around 0.038 mm intensively. For the AC2, the particle size from 0.045 mm to 0.212 mm accounts for 95.40 %. The particle size of AC3 ranges from 0.090 mm to 0.355 mm and distribute around 0.212 mm. With regard to AC4, the particle size varies from 0.18 mm to 0.5 mm and distribute in 0.355mm intensively. The average particle size of AC1-AC4 are 0.0342mm, 0.1015 mm, 0.2103 mm and 0.3815 mm, respectively.

FTIR spectroscopy of various adsorbents shown in Fig. 2, there is no significant change observed for the species of functional group for all the adsorbents. However, the peak area of the four adsorbents have slight differences. A broad band between 3100 and 3700 cm^{-1}, peak at about 3400 cm^{-1}, indicates a slight decrease from AC1 to AC4 in relative intensity of the hydroxyl content, which may hinder the adsorption of quinoline. Because the quinoline solution is weak alkaline. There is a band between 2800-3000 cm^{-1} ,with dominate peak at 2922cm^{-1}, which corresponds to aliphatic carbon groups (Guo and Bustin 1998), and the peak area shows no obvious change in all adsorbents. The peak at 1600 cm^{-1} corresponds to aldehydes and ketone groups (Ledesma et al. 1998). The FTIR spectra of the samples show transmittance in the 1032 cm^{-1} region due to the ash, such as kaolin (Zhu 2001) and the AC1 is larger than other adsorbents in relative intensity of the ash content. The peak at 550 cm^{-1} may be attributed to S-S in aromatics(Sarkar et al. 2007).

Fig.3 shows the XRD profiles of the four adsorption. The peak and peak area of the four adsorbents are similar. There are kaolin, montmorillonite, quartz, calcium oxide, illites, iron silicide and aluminum bentonite in the adsorbents.

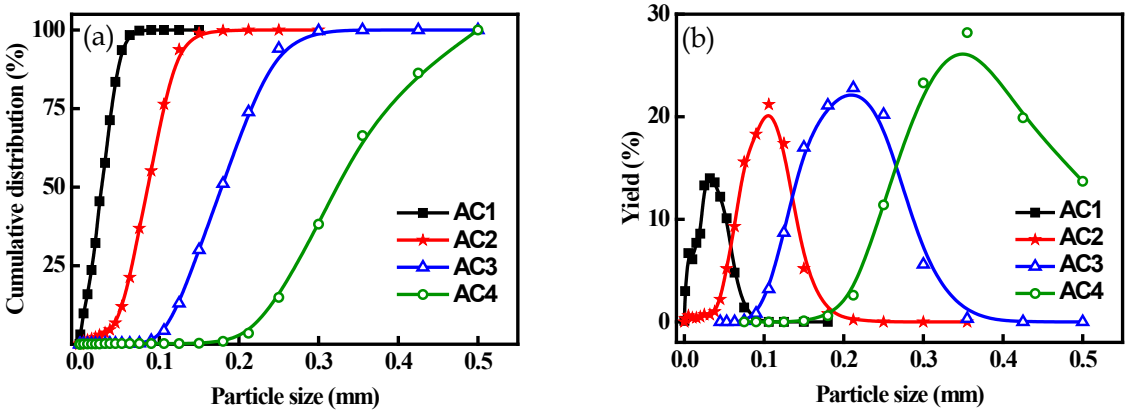

Fig. 1. The particle size of various adsorbents

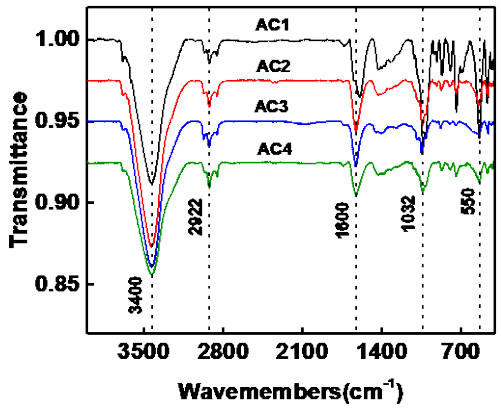

Fig. 2. FTIR spectroscopy of various adsorbents

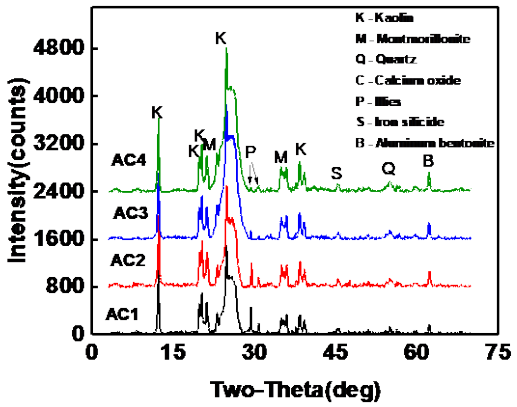

Fig. 3. X-ray diffraction patterns of all the adsorbents

The ash content of the four adsorbents were presented in Table 1. With the particle size increasing, the ash content decreases. Because the clay minerals are easily argillized.

The specific surface areas were calculated using the BET model (Kaya et al. 2013a), and the specific surface areas were 3.5 $m^2 \cdot g^{-1}$, 1.5 $m^2 \cdot g^{-1}$, 0.7 $m^2 \cdot g^{-1}$, 0.1 $m^2 \cdot g^{-1}$ respectively, which decrease with the particle size increasing. The specific surface area can provide adsorption sites for quinoline. As can be seen in Fig. 4, the pore size distribution was calculated in the standard manner by using BJH method(Barrett et al. 1951). There is a significant decrease in mesoporous from AC1 to AC4, which will affect the adsorption capacity. However, the AC2 has more megalopore than AC1, which may control the diffuse rate.

Table 1. The ash content of all adsorbents

Samples	AC1	AC2	AC3	AC4
Ash content/ %	9.88	9.54	9.16	9.04

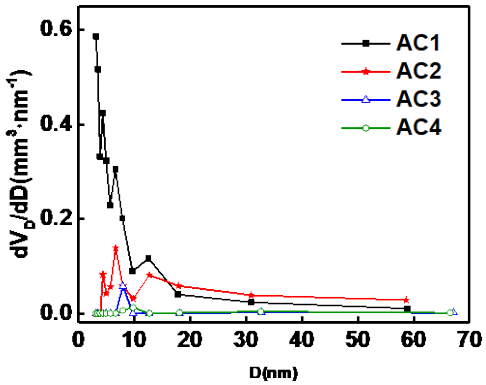

Fig. 4. The distribution curves of mesoporous and megalopore for all adsorbents

3.2 Adsorption experiments

3.2.1 Effect of contact time on the adsorption capacity

The effect of contact time (t) on the adsorption capacity of quinoline by different adsorbents is shown in Fig. 5. The contact time curve of AC1 shows that the removal efficiency increases quickly before 60 min. The curves of AC3 and AC4 present rise slowly with time going before 60 min and the increase trend of AC1 is faster, for bigger specific surface providing more adsorption site. They reached quasi-equilibrium after 120 min, beyond which there was no significant increase in removal. The adsorption capacity of AC1-AC4 are 1.22 mg ·g^{-1}, 0.73 mg ·g^{-1}, 0.40 mg ·g^{-1}, 0.28 mg ·g^{-1} respectively and the removal efficiency are 97.62%, 58.11%, 32.00%, 22.54% respectively.

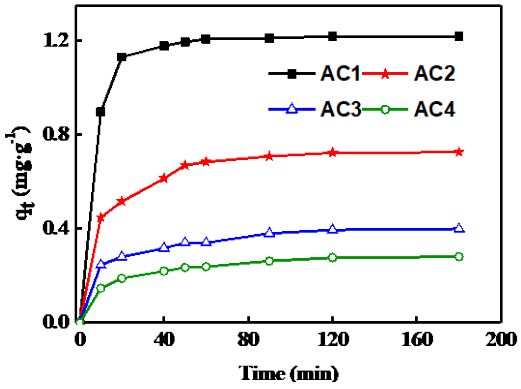

Fig. 5. Effect of contact time on the adsorption capacity of quinoline by various adsorbents

3.2.2 Relation between specific surface area and adsorption capacity

The adsorption capacity verses specific surface area curve presented in Fig. 6. There is a fitting straight line, and the correlation coefficient is 0.98366, which indicates that adsorption capacity presents a linear increase with the increase of specific surface area. The activated carbon adsorb organic contaminants from aqueous solution also presented the similar change trend investigated by Li et al. (2002).

3.3. Adsorption kinetics study

The data of adsorption experiments were analyzed by the function of origin 8.0 linear fitting using the pseudo-first-order model, pseudo-second-order model, Intra-particle diffusion showed in the Fig. 7, the kinetics parameters and the correlation coefficient calculated by the intercept and slope are shown in Table 1.

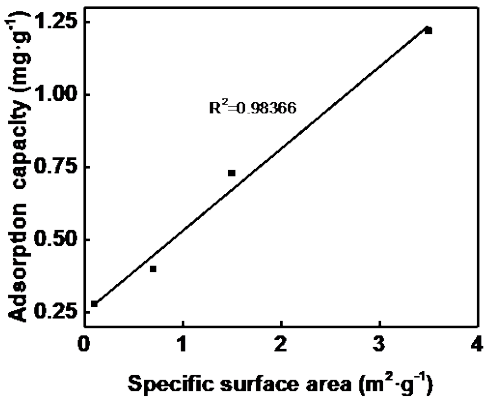

Fig. 6. The adsorption capacity verses specific surface area curve

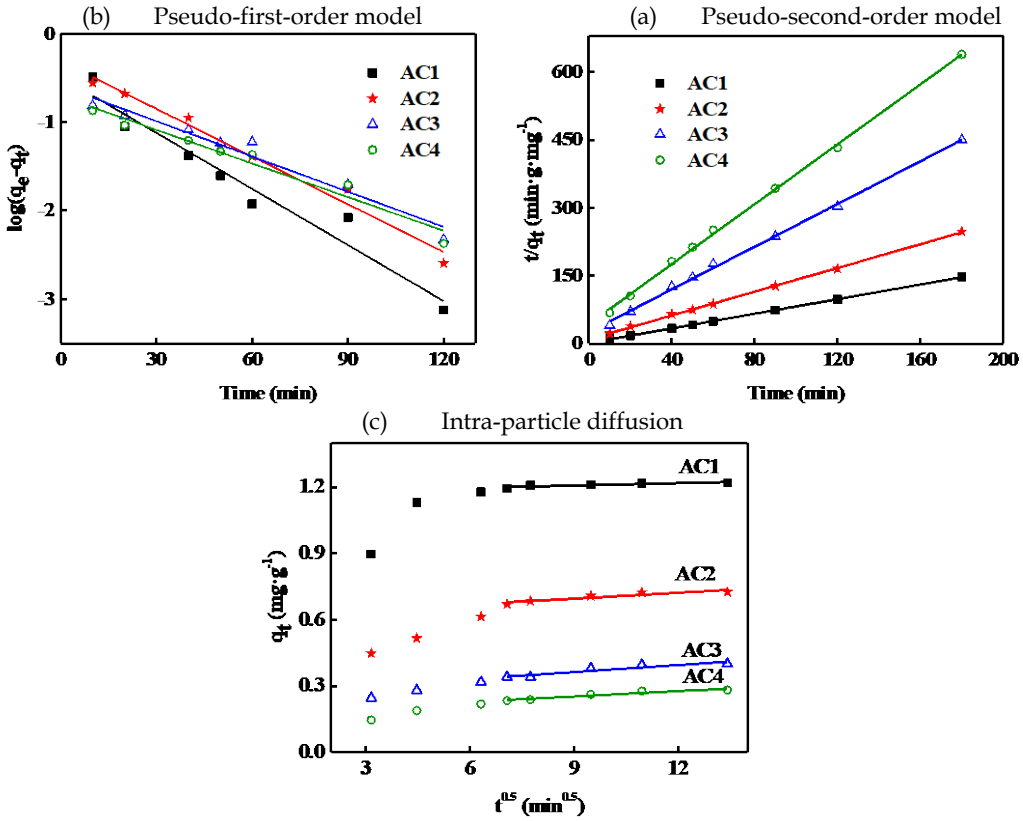

Fig. 7. Three kinds of kinetic plots for quinoline by various adsorbents

3.3.1. Pseudo-first-order model

According to Table 1, the removal rate from high to low follows the order： AC1, AC2, AC3, AC4, which is similar with the specific surface area order. The $q_{e,\ meas}$ values are far bigger than the $q_{e,\ calc}$, and the correlation coefficient are not the biggest comparing with pseudo-second-order model. So that the pseudo-first-order model provided a poor fit to the experimental data.

3.3.2. Pseudo-second-order model

From the Table 2, the pseudo-second-order rate expression yielded correlation coefficients between 0.9982 and 0.9998 and provided a good fit for all adsorbents. The pseudo-second-order rate equation also yielded $q_{e,calc}$ values close to the obtained $q_{e,meas}$ results (Table 2). Therefore, sorption of quinoline onto the anthracite is most appropriately approximated by the pseudo-second-order model, which

indicates that the adsorption process belongs to chemical adsorption. The result is similar with some results studied by many authors. Ugurlu et al.(Ugurlu et al. 2005) described the removal of phenolics by using fly ash and concluded that the pseudo-second-order rate expression best descried the kinetic data, which determined that the adsorption mechanism was chemical adsorption. Srivastava et al.(Srivastava et al. 2005) concluded that the pseudo-second-order rate model best described the sorption of chemical oxygen demand (COD) from pulp and paper mill wastewater onto bagasse fly ash; the predominant sorption process was chemisorption. Kerstin I. Andersson et al. (Andersson et al. 2011b) studied the adsorption of lignin onto activated charcoal and fly ash followed pseudo-second-order rate kinetics.

Table 2. Kinetics parameters for the removal of quinoline by different adsorbents

Adsorbents	**Pseudo-first-order model**			
	$q_{e,meas}$/ mg ·g^{-1}	$q_{e,calc}$/ mg ·g^{-1}	K_1/ min^{-1}	R^2
AC1	1.22	0.33	0.0486	0.9513
AC2	0.73	0.49	0.0415	0.9806
AC3	0.40	0.26	0.0306	0.9597
AC4	0.28	0.20	0.0292	0.9615
Adsorbents	**Pseudo-second-order model**			
	$q_{e,calc}$/ mg ·g^{-1}	K_2/ g ·mg^{-1} ·min^{-1}	h/ mg ·g^{-1} ·min^{-1}	R^2
AC1	1.24	0.3525	0.5419	0.9998
AC2	0.76	0.3082	0.1796	0.9994
AC3	0.42	0.2699	0.0486	0.9982
AC4	0.30	0.2497	0.0228	0.9988
Adsorbents	**Intra-particle diffusion**			
	K_3/ mg ·g^{-1} ·min$^{-0.5}$		I/ mg g^{-1}	R^2
AC1	0.0335		0.9134	0.6253
AC2	0.0274		0.4226	0.7981
AC3	0.0157		0.2150	0.9223
AC4	0.0129		0.1302	0.8985

3.3.3. Intra-particle diffusion model

According to Eq. (7), a plot of q_t versus $t^{0.5}$ should be a straight line with a slope K_3 and intercept I when adsorption mechanism follows the intra-particle diffusion process. Fig. 8 presents a plot of q_t versus $t^{0.5}$ for all the adsorbents. It indicates that adsorption process of quinoline onto different particle sizes of anthracite can divide into two linear equations, i.e. it includes initial rapid diffusion and subsequent slow internal diffusion (Allen et al. 1989, Fierro et al. 2008). As can be seen from Fig. 8, the smaller particle size has the faster and shorter rapid diffusion, and the curve of AC4 is almost a straight line. The similar conclusion was conducted by Qiang Zhou, who studied that removal of mercury by using activated carbon (Qiang et al. 2013). The value of I gives an idea about the thickness of the boundary layer, i.e. the larger intercept the greater is the boundary layer effect (Mohan and Karthikeyan 1997). The deviation of the straight lines from the origin may be due to the difference in the rate of mass transfer during the initial and final stages of adsorption(Fierro et al. 2008). It also indicates that the pore diffusion is not the rate-controlling step(Wu and Yu 2006).

3.4. Adsorption equilibrium research

The data of adsorption equilibrium was analyzed using Origin 8.0 linear fitting using Freundlich isotherm and Langmuir isotherm. The isotherm parameters and the correlation coefficient calculated by

the intercept and slope are shown in the Table 3.

3.4.1. Langmuir isotherms

Fig. 9 (a) shows the plot of C_e/q_e against C_e for testing of the Langmuir isotherm at 25℃. According to the Table 3, the value of q_m in 25 ℃ is larger than the experimental value, which indicated that Freundlich model dose not provided a good fit for all adsorbents. The values of R_L[a] used to describe the process favorability and adsorption capacity (Andersson et al. 2011a). The R_L[a] values were all between 0 and 1 indicating a favorable sorption process.

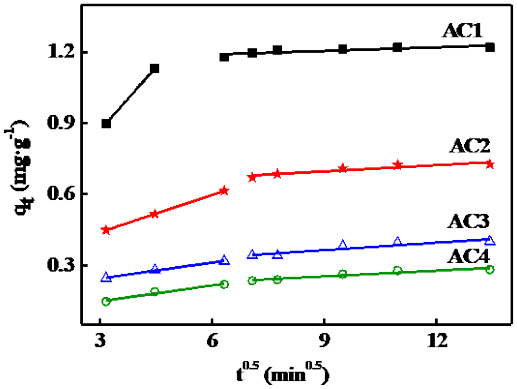

Fig. 8. Weber and Morris intra- particle diffusion plots for the removal of quinoline by various adsorbents

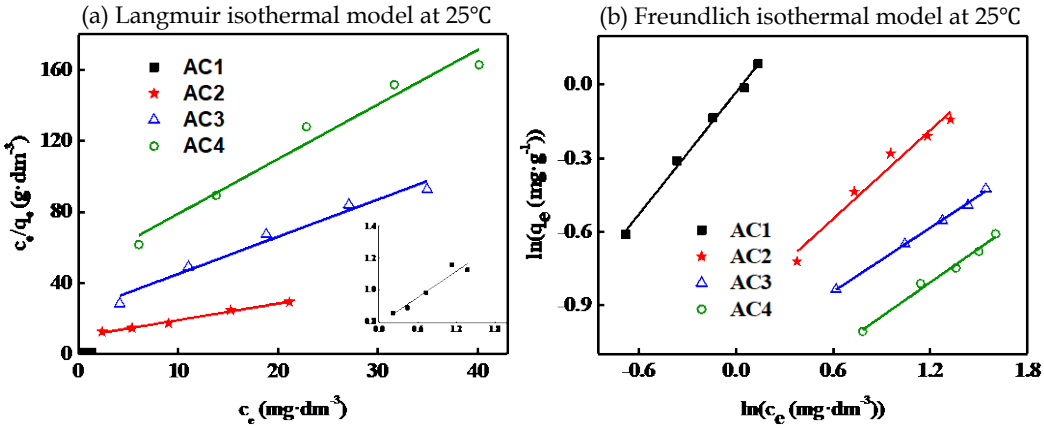

Fig. 9. Linear fitting of adsorption equilibrium of quinoline on adsorbents

3.4.2. Freundlich isotherm

Fig. 9 (b) shows the plot of lnq_e against lnc_e for testing of the Freundlich isotherm at 25 ℃. According to the Table 3, the correlation coefficients of Freundlich model are also closer to unity from 0.9486 to 0.9980 and provided a good fit for all adsorbents. That indicates nonuniformity of anthracite surface and adsorption of quinoline by using the four adsorbents belongs to chemical adsorption, which corresponds with kinetic conclusion. The 1/n is used to evaluate of adsorption superiority (Dabrowski et al. 1983). The values of 1/n are between 0.4 and 0.9, which indicated that they adsorb easily. This was supported by the R_L[a] less than 1 obtained from the Langmuir isotherm. The values of K_{Fr} in the 50℃ is larger than that in the 25 ℃, which indicated the adsorption process belongs to endothermic reaction. Kerstion I et al. showed that adsorption of lignin from wastewater by using activated carbon is endothermic(Andersson et al. 2011a), which was supported by Mall et al. (Mall et al. 2005)

4. Conclusions

In this work, removal of quinoline using anthracite of various particle sizes was studied. The adsorption capacity presents a linear increase with the increase of specific surface area, which is similar with Lei

Li's study (Li et al. 2002). The AC1 possessing biggest adsorption capacity and removal efficiency are 1.22 mg·g^{-1} and 97.62% respectively. The adsorption of quinoline onto various particle size of anthracite occurs by chemical adsorption, and the rate of adsorption could be controlled by several processes simultaneously. The result has been confirmed by several scholars (Andersson et al. 2011b, Srivastava et al. 2005, Ugurlu et al. 2005, Wu and Yu 2006). The adsorption process are endothermic, which corresponds with removal of malachite green dye and lignin using activated carbon (Andersson et al. 2011a, Mall et al. 2005). The R_L[a] values and the 1/n indicate that the adsorption is a favorable sorption process (Dabrowski et al. 1983). Adsorption process of quinoline onto different sizes of anthracite includes initial rapid diffusion and subsequent slow internal diffusion. The smaller particle size had the faster and shorter rapid diffusion, which was confirmed by Qiang Zhou who had obtained the same conclusion (Qiang et al. 2013).

Table 3. Isotherm parameters for removal of quinoline by various adsorbents

Absorbents	**Langmuir model**				
	T/℃	K_L/dm^3·mg^{-1}	q_m/ mg g^{-1}	R_L[a]	R^2
AC1	25	4.6181	3.66	0.004	0.8998
	50	6.2807	2.16	0.003	0.9264
AC2	25	0.1097	1.08	0.154	0.9889
	50	0.5649	1.22	0.034	0.9976
AC3	25	0.0198	0.48	0.503	0.9663
	50	0.0384	0.65	0.342	0.9979
AC4	25	0.0067	0.32	0.748	0.9569
	50	0.0132	0.41	0.603	0.9874
Absorbents	**Freundlich model**				
	T/℃	K_{Fr}/ dm^3·mg^{-1}		1/n	R^2
AC1	25	0.9292		0.8314	0.9951
	50	1.3228		0.6779	0.9931
AC2	25	0.1230		0.6036	0.9698
	50	0.3330		0.5037	0.9486
AC3	25	0.0785		0.4349	0.9980
	50	0.0899		0.5060	0.9830
AC4	25	0.0434		0.4629	0.9879
	50	0.0601		0.4601	0.9909

Acknowledgements

This work was supported by the supported by National Natural Science Foundation of China (NO. 51604280 and 51504262).

References

AKSU, Z. & J. YENER, 2001. *A comparative adsorption/biosorption study of mono-chlorinated phenols onto various sorbents*. Waste Manage (Oxford), 21, 695-702.

ALLEN, S. J., G. MCKAY & K. Y. H. KHADER, 1989. *Intraparticle diffusion of a basic dye during adsorption onto*

sphagnum peat. Environ Pollut, 56, 39-50.

ANDERSSON, K. I., M. ERIKSSON & M. NORGREN, 2011a. *Removal of lignin from wastewater generated by mechanical pulping using activated charcoal and fly ash: Adsorption isotherms and thermodynamics*. Industrial & Engineering Chemistry Research, 50, 7722-7732.

ANDERSSON, K. I., M. ERIKSSON & M. NORGREN, 2011b. *Removal of lignin from wastewater generated by mechanical pulping using activated charcoal and fly ash: adsorption kinetics*. Industrial & Engineering Chemistry Research, 50, 7733-7739.

BADMUS, M. & T. AUDU, 2009. *Periwinkle shell: Based granular activated carbon for treatment of chemical oxygen demand (COD) in industrial wastewater*. The Canadian Journal of Chemical Engineering, 87, 69-77.

BARRETT, E. P., L. G. JOYNER & P. P. HALENDA, 1951. *The determination of pore volume and area distributions in porous substances. I. Computations from nitrogen isotherms*. J Am Chem Soc, 73, 373-380.

BAŞAR, C. A., 2006. *Applicability of the various adsorption models of three dyes adsorption onto activated carbon prepared waste apricot*. J Hazard Mater, 135, 232-241.

BURMISTRZ, P., A. ROZWADOWSKI, M. BURMISTRZ & A. KARCZ, 2014. *Coke dust enhances coke plant wastewater treatment*. Chemosphere, 117, 278-284.

CAI, C.-F. & C.-G. TANG, 2012. *Competitive adsorption of main organic pollutants from coking wastewater on coking coal*. Journal of China Coal Society, 37, 1753-1759.

CAI, C., X. ZHENG, H. GAO & M. ZUO, 2010. *Adsorption kinetics of organic in coking wastewater effluent from secondary sedimentation tank on coal*. Journal of China Coal Society, 35, 299-302.

CARVAJAL-BERNAL, A. M., F. GóMEZ, L. GIRALDO & J. C. MORENO-PIRAJáN, 2015. *Adsorption of phenol and 2, 4-dinitrophenol on activated carbons with surface modifications*. Microporous Mesoporous Mater, 209, 150-156.

CHANGBIN XIA, X. H., 2000. *Adsorption heavy metal ion by using sulfonated lignite*. Material Protection, 33, 19-20.

CHATZOPOULOS, D., A. VARMA & R. L. IRVINE, 1993. *Activated carbon adsorption and desorption of toluene in the aqueous phase*. AlChE J, 39, 2027-2041.

DABROWSKI, A., M. JARONIEC & J. TóTH, 1983. *Application of tóth's equation to describe the single-solute adsorption from dilute solutions on solids*. J Colloid Interface Sci, 94, 573-576.

FANG, J., X. SONG, C. CAI & C. TANG, 2010. *Adsorption characteristica of coking coal in coking wastewater treatment*. Jounal of Anhui Univercity of Technology and Science, 25, 43-47.

FIERRO, V., V. TORNé-FERNáNDEZ, D. MONTANé & A. CELZARD, 2008. *Adsorption of phenol onto activated carbons having different textural and surface properties*. Microporous Mesoporous Mater, 111, 276-284.

FLETCHER, A. J., Y. UYGUR & K. M. THOMAS, 2007. *Role of surface functional groups in the adsorption kinetics of water vapor on microporous activated carbons*. The Journal of Physical Chemistry C, 111, 8349-8359.

GERENTE, C., V. LEE, P. L. CLOIREC & G. MCKAY, 2007a. *Application of chitosan for the removal of metals from wastewaters by adsorption – mechanisms and models review*. Critical reviews in environmental science and technology, 37, 41-127.

GERENTE, C., V. K. C. LEE, P. L. CLOIREC & G. MCKAY, 2007b. *Application of Chitosan for the Removal of Metals From Wastewaters by Adsorption – Mechanisms and Models Review*. Critical Reviews in Environmental Science and Technology, 37, 41-127.

GUO, Y. & R. BUSTIN, 1998. *FTIR spectroscopy and reflectance of modern charcoals and fungal decayed woods: implications for studies of inertinite in coals*. International Journal of Coal Geology, 37, 29-53.

HO, Y.-S. & G. MCKAY, 1999. *Pseudo-second order model for sorption processes*. Process Biochem, 34, 451-465.

HO, Y., J. PORTER & G. MCKAY, 2002. *Equilibrium isotherm studies for the sorption of divalent metal ions onto peat: copper, nickel and lead single component systems*. Water, Air, Soil Pollut, 141, 1-33.

KAYA, E. M. Ö., A. S. ÖZCAN, Ö. GöK & A. ÖZCAN, 2013a. *Adsorption kinetics and isotherm parameters of naphthalene onto natural- and chemically modified bentonite from aqueous solutions*. Adsorption, 19, 879-888.

KAYA, E. M. Ö., A. S. ÖZCAN, Ö. GöK & A. ÖZCAN, 2013b. *Adsorption kinetics and isotherm parameters of naphthalene onto natural-and chemically modified bentonite from aqueous solutions*. Adsorption, 19, 879-888.

LEDESMA, E. B., P. F. NELSON & J. C. MACKIE. 1998. The formation of nitrogen species and oxygenated PAH during the combustion of coal volatiles. In *Symposium (International) on Combustion*, 1687-1693. Elsevier.

LI, L., P. A. QUINLIVAN & D. R. KNAPPE, 2002. *Effects of activated carbon surface chemistry and pore structure on the adsorption of organic contaminants from aqueous solution*. Carbon, 40, 2085-2100.

MAGNUS, E., G. E. CARLBERG & H. HOEL, 2000. *TMP wastewater treatment, including a biological high-efficiency compact reactor: Removal and characterization of organic components*. Nord Pulp Pap Res J, 15, 29-36.

MALL, I. D., V. C. SRIVASTAVA, N. K. AGARWAL & I. M. MISHRA, 2005. *Adsorptive removal of malachite green dye from aqueous solution by bagasse fly ash and activated carbon-kinetic study and equilibrium isotherm analyses*. Colloids and Surfaces A: Physicochemical and Engineering Aspects, 264, 17-28.

MOHAN, S. V. & J. KARTHIKEYAN, 1997. *Removal of lignin and tannin colour from aqueous solution by adsorption onto activated charcoal*. Environ Pollut, 97, 183-187.

POLAT, H., M. MOLVA & M. POLAT, 2006. *Capacity and mechanism of phenol adsorption on lignite*. Int J Miner Process, 79, 264-273.

QIANG, Z., D. YUFENG, M. YONGQIU & Z. CHUN, 2013. *Kinetics and mechanism of activated carbon adsorption for mercury removal*. Proceedings of the CSEE 33, 10-17.

SARKAR, M., A. SARKAR & J. GOSWAMI, 2007. *Mathematical modeling for the evaluation of zinc removal efficiency on clay sorbent*. J Hazard Mater, 149, 666-674.

SRIVASTAVA, V. C., I. D. MALL & I. M. MISHRA, 2005. *Treatment of pulp and paper mill wastewaters with poly aluminium chloride and bagasse fly ash*. Colloids and Surfaces A: Physicochemical and Engineering Aspects, 260, 17-28.

SUTTON, S. D., S. L. PFALLER, J. R. SHANN, D. WARSHAWSKY, B. K. KINKLE & J. R. VESTAL, 1996. *Aerobic biodegradation of 4-methylquinoline by a soil bacterium*. Applied and environmental microbiology, 62, 2910-2914.

UGURLU, M., A. GURSES, M. YALCIN & C. DOGAR, 2005. *Removal of phenolic and lignin compounds from bleached kraft mill effluent by fly ash and sepiolite*. Adsorption, 11, 87-97.

WU, J. & H.-Q. YU, 2006. *Biosorption of 2, 4-dichlorophenol from aqueous solution by Phanerochaete chrysosporium biomass: Isotherms, kinetics and thermodynamics*. J Hazard Mater, 137, 498-508.

YI, D. 2012. Study on copper adsorption on Shanxi Pingsuo weathered coal. Chinese Academy of Agricultural Sciences.

ZHU, H., LI, HU LIN , OU, ZHESHEN , WANG, DIANZUO, XIAOLI LV, 2001. *Study on surface modification of different rank coals by using FTIR*. Journal of China University of Mining & Technology, 30, 366-370.